Mifepristone, a Blocker of Glucocorticoid Receptors, Promotes Photoreceptor Death

Marisa A. Cubilla, Vicente Bermúdez, Melisa D. Marquioni Ramella, Tomás P. Bachor, and Angela M. Suburo

Purpose. Glucocorticoids are best known by their protective effect on retinal photoreceptor damage. However, they could also be involved in photoreceptor homeostasis under basal, nonstressful conditions. Therefore, we aimed to study glucocorticoid-induced changes of survival-related molecules in male mice retinas under standard illumination conditions (12 hours light, $\leq$ 60 lux/12 h dark).

Methods. Male Balb-c mice were injected with dexamethasone (DEX), a selective glucocorticoid receptor α (GRα) agonist, its antagonist mifepristone (MFP), or both drugs (D+M) at noon. A group of mice was subjected to surgical adrenalectomy (AdrX). Retinas were studied by histology, immunohistochemistry, TUNEL procedure, and Western blotting at different periods after pharmacological or surgical intervention (6 hours, 48 hours, or 7 days).

Results. The antiapoptotic molecule Bcl-X_L significantly increased 6 hours after DEX injection. By contrast, this molecule could no longer be found after MFP injection. At the same time, high levels of cleaved caspase-3 (CC-3) and Bax appeared in retinal extracts, and TUNEL$^+$ nuclei selectively showed in the outer nuclear layer (ONL). After MFP, retinal extracts also contained phosphorylated histone H2AX (p-H2AX), a marker of DNA breakage and repair. Loss of ONL nuclear rows and decrease of rhodopsin levels were evident 7 days after MFP administration. These changes were minimized when DEX was given together with MFP (D+M). In the absence of MFP, DEX increased Bcl-X_L in every retinal layer, with a marked intensification in photoreceptor inner segments. Numerous TUNEL$^+$ nuclei rapidly appeared in the ONL after AdrX.

Conclusions. A single dose of MFP induced selective photoreceptor damage in the absence of other environmental stressors. Because damage was prevented by DEX, and was reproduced by AdrX, our findings suggest that glucocorticoids play a critical role in photoreceptor survival. (*Invest Ophthalmol Vis Sci.* 2013;54:313–322) DOI:10.1167/iovs.12-10014

From Medicina Celular y Molecular, Facultad de Ciencias Biomédicas, Universidad Austral, Pilar, Argentina.

Supported by Universidad Austral and ANPCyT (PICTO-AUSTRAL 2008-00090).

Submitted for publication April 11, 2012; revised September 21 and November 10, 2012; accepted November 26, 2012.

Disclosure: **M.A. Cubilla**, None; **V. Bermúdez**, None; **M.D. Marquioni Ramella**, None; **T.P. Bachor**, None; **A.M. Suburo**, None

Corresponding author: Angela M. Suburo, Facultad de Ciencias Biomédicas, Universidad Austral, Pilar B1629AHJ, Buenos Aires, Argentina; amsuburo@cas.austral.edu.ar.

Glucocorticoids are widely used in various ophthalmological conditions,[1] such as traumatic optic neuropathy,[2] diabetic macular edema,[3] retinal vein occlusion,[4] cystoid macular edema,[5,6] noninfectious uveitis,[7] radiation retinopathy,[8] and even for AMD in the combination known as triple therapy.[9] Evidence for the role of these steroids in photoreceptor protection derives from experimental retinal degeneration studies. In the light-induced degeneration model in rodents, glucocorticoid-mediated protection has been associated to a decrease of lipid peroxidation[10] or to suppression of the activator protein 1 (AP-1) upregulation.[11] However, glucocorticoids can prevent AP-1 increases without avoiding photoreceptor damage.[12] Additionally, glucocorticoid treatment increases photoreceptor survival after laser-induced damage.[13,14] Intravitreal fluocinolone acetonide protects photoreceptors in Royal College of Surgeons (RCS) rats and simultaneously reduces microglial activation.[15]

On the other hand, we have previously shown that mifepristone (MFP, RU 486), an antagonist of glucocorticoid α receptors (GRα), aggravates light-induced retinal damage.[16] In this model, MFP administration increases cleaved caspase-3 (CC-3) in photoreceptor nuclei and rhodopsin (RHO) depletion. Dexamethasone (DEX), a well-known GRa ligand,[1] prevents light-induced CC-3 activation and RHO reduction, both in control and MFP-treated mice.[16] Preliminary experiments showed that MFP induced selective death of murine photoreceptors under standard illumination conditions (12 hours light, $\leq$ 60 lux/12 h dark), without detectable injury to other retinal cells (Cubilla MA, et al. *IOVS* 2011;52: ARVO E-Abstract 5462). Hence, we have now explored the effects of MFP and adrenalectomy (AdrX) on photoreceptor survival in the absence of known environmental stressors.

Several mechanisms have been proposed to explain the role of glucocorticoids as key signals in the balance between survival and death of diverse cell phenotypes.[17,18] Glucocorticoid-dependent death or survival is directly associated with the selective expression of the short or long isoforms of Bcl-X (Bcl-X_S or Bcl-X_L), which are pro- and antiapoptotic, respectively.[17] Cells resistant to glucocorticoid-induced apoptosis, such as some cancer cells[19,20] and fibroblasts,[21] show increased production of Bcl-X_L. In the hippocampus, where they induce cell death, glucocorticoids increase the ratio of the proapoptotic molecule Bax relative to the antiapoptotic molecule Bcl-X_L.[22] Therefore, we used the ratio Bcl-X_L/Bax to evaluate the role of glucocorticoids under our experimental conditions.

Materials and Methods

Animals

Experimental design, reviewed and approved by our Institutional Animal Care and Use Committee, followed the standards of the ARVO

Table 1. Primary Antibodies Used in Immunohistochemistry and Western Blots

Antibody	Type	Source
GAPDH	Mouse monoclonal	(6C5, sc-32233) Santa Cruz Biotechnology, Inc., Santa Cruz, CA
Bcl-X	Rabbit polyclonal	(B9304) Sigma-Aldrich, St. Louis, MO
Bax	Rabbit polyclonal	(sc-493) Santa Cruz Biotechnology, Inc.
CC-3	Rabbit polyclonal	(9661) Cell Signaling Technology, Inc., Danvers, MN
p-H2AX	Rabbit monoclonal	(ab2893) Abcam, Inc., Cambridge, MA
RHO	Mouse monoclonal	(B6-30) J. Nathans (School of Medicine, Johns Hopkins University, Baltimore, MD)

Statement for the Use of Animals in Ophthalmic and Vision Research. We used male BALB/c mice, between 35 to 45 days of age. One of the experiments was repeated in C57Bl6/J mice of the same age and sex (see below). Mice were bred under standard cycling illumination conditions (12 hours light, $\leq$ 60 lux/12 h dark). Experiments began at 12 AM, with a 24-hour period of complete darkness for all mice. At noon on the next day, we randomly separated them into the different experimental groups and returned them to the standard light cycle. These animals were euthanatized 6 hours, or 2 or 7 days after pharmacological intervention.

Pharmacological Interventions

We used MFP (Sigma-Aldrich, St. Louis, MO) in propylene glycol and dexamethasone disodium phosphate (DEX; Sidus, Buenos Aires, Argentina) in NaCl 0.9% solution as subcutaneous injections. Mice received a single initial dose of 10 mg/kg MFP or 4 mg/kg/d DEX during 2 consecutive days. Some mice were given different doses, as specified in the text or figure captions. For combined treatment (D+M), mice received both drugs simultaneously but in different injections. Nontreated controls received the same volumes of both vehicles (VHCs). MFP-treated mice received a glucose supplement (1 mL of 5% glucose, intraperitoneal; Fidex, Buenos Aires, Argentina) to prevent a stress-like condition arising in these animals.

Adrenalectomy

Mice were anesthetized with desfluorane and surgery was performed according to conventional procedures.[23] We ablated both adrenals together with the perirenal fat pad, and confirmed extraction microscopically. The abdominal wall and the skin were sutured separately. Sham animals were anesthetized and had a skin incision. All animals received antibiotics (20 mg/kg/d ceftazidime; Fada Pharma, Buenos Aires, Argentina) during 2 days. A 0.9% NaCl solution replaced drinking water for adrenalectomy (AdrX) mice.

Immunohistochemical and TUNEL Procedures

After deep anesthesia, animals were perfused transcardially with 4 g/100 mL paraformaldehyde in a phosphate buffer 0.1 M, pH 7.3. Dorsolateral regions of the eyeball were ink-labeled before enucleation. After lens removal, fixation continued during 1 hour. Sucrose solutions of increasing concentrations (5%–20% in phosphate buffer 0.01 M) provided cryoprotection. Eye pairs (one control and one experimental) were embedded in the optimal cutting temperature compound (OCT; Biopack, Buenos Aires, Argentina) and frozen in N2 cooled acetone. Eyes were sectioned through para-equatorial planes; thus, each section crossed the temporal and nasal retinas. Cryosections (9-μm thick) were mounted on gelatinized slides and, after dehydration and delipidization, they were incubated with primary antibodies (Table 1). Detection was made with biotinylated secondary antibodies, followed by the avidin-biotin-peroxidase complex (Elite Vector; Vector Laboratories, Burlingame, CA) that was developed with a nickel-enhanced procedure.[24] In negative controls, diluent replaced the primary antibody.

Alternatively, 6-μm sections collected on positive slides (Instrumental Pasteur, Argentina) were assayed for DNA fragmentation with the FragEL system (DNA Fragmentation Detection Kit, Fluorescent-TdT Enzyme, Calbiochem; Merck KGaA, Darmstadt, Germany). Labeled nuclei were scored by a blinded operator.

Evaluation of the Outer Nuclear Layer in Neutral Red–Stained Sections

Eyes were embedded as before and seriate sections were stained with 0.2% Neutral Red (Sigma-Aldrich) for 8 minutes. The thickness of the outer nuclear layer (ONL) was evaluated in sections through the optic nerve head (ONH), using digital images obtained with a Nikon-DS digital camera (Nikon, Microlat, Argentina) at ×4 magnification with 2560 × 1920 pixels.[25] Measurements were made at 250-μm intervals from the ONH with the tools of Adobe Photoshop CS4 Extended (Adobe, San Jose, CA).

Western Blots

At the end of the experiment, animals underwent 30 minutes of complete darkness to allow full separation of the RPE. Euthanasia and enucleation took place under dim red light. Retinas (6 per experimental point) were extracted in a buffer containing 5 mM Tris-HCl with 2 mM $MgCl_2$, 2 mM EDTA, 65 mM NaCl, 1% Triton X-100, and protease inhibitor cocktail (Sigma-Aldrich). After measuring protein concentration with the Bradford protein assay (Sigma-Aldrich), samples (30 μg protein per lane) were separated by SDS-PAGE (BioRAD, Canton, MA). They were transferred (120 v, 120 minutes) to nitrocellulose filters (Hybon-P; Amersham Pharmacia Biotech, Piscataway, NJ) using standard techniques. Membranes were incubated with primary antibodies (Table 1), followed by appropriate biotinylated secondary antibodies and extravidin-peroxidase (Sigma-Aldrich). Immunoreactive bands were developed with an enhanced chemiluminescence detection kit (ECL; Amersham Pharmacia Biotech). Outcomes were pixels per band, measured with Adobe Photoshop CS4 Extended (Adobe), using automatic adjustment and measurement sequences. Labeling of glyceraldehyde-3-phosphate dehydrogenase (GAPDH) bands confirmed equal transfer to the membranes.

Statistics

Quantitative data are presented as average ± SE, with an indication of the number of samples for each experiment in the text or the corresponding figure legends. Student's *t*-test or ANOVA, complemented by Tukey's test for multiple comparisons, were calculated with GraphPad Prism 5.00 for Windows (GraphPad Software, San Diego CA; www.graphpad.com). Letters shared by two or more groups indicate lack of significant statistical difference between those groups.

Results

CC-3 Under Basal Illumination Conditions

Control retinas did not show any CC-3 protein. By contrast, injection of 4, 10, or 30 mg/kg MFP provoked the appearance of increasing levels of CC-3 just 6 hours after MFP administra-

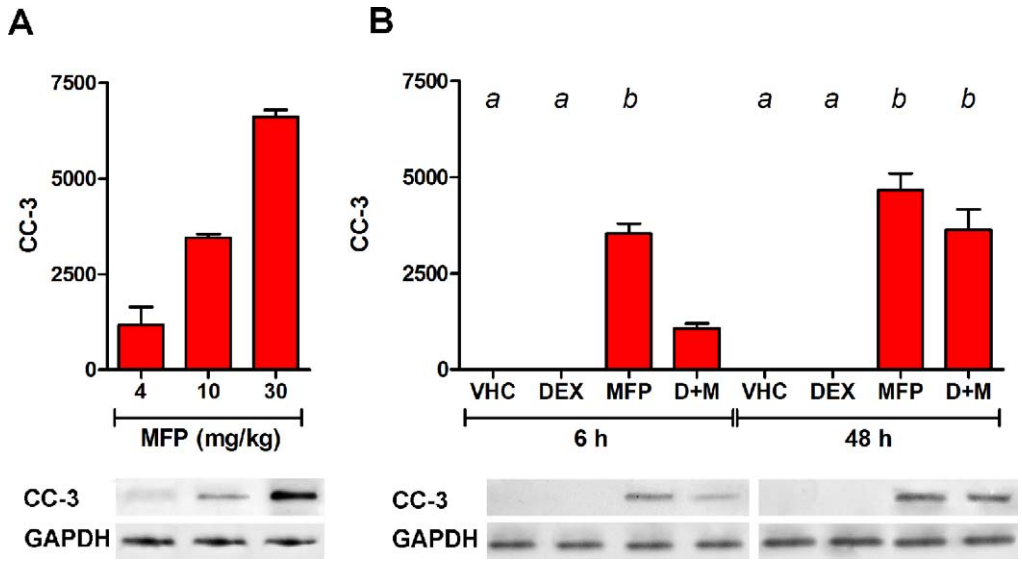

Figure 1. Levels of CC-3 protein in retinal extracts after different pharmacological interventions. In all figures, a shared letter indicates lack of significant statistical differences. (**A**) Increasing CC-3 levels appeared 6 hours after administration of increasing MFP doses, from 4 to 30 mg/kg (ANOVA, $P < 0.0001$; $n = 3$, $P < 0.01$ for all comparisons). *Bottom*: representative proteinograms showing CC-3 and GAPDH bands from the same extracts. (**B**) Levels of CC-3 appearing after DEX (4 mg/kg/d), MFP (10 mg/kg, single dose) or their combination, D+M. After 6 and 48 hours, CC-3 protein was present only in mice treated with MFP or D+M. Co-administration of DEX reduced CC-3 levels at 6 hours ($P < 0.001$) but did not prevent their increase at 48 hours. Below, CC-3 and GAPDH bands from a representative WB.

tion (Fig. 1A). Therefore, in further experimental work we used a single 10-mg/kg injection of MFP at the beginning of the experiment.

We then compared DEX and MFP effects at 6 and 48 hours. CC-3 was not found at any time in animals receiving VHC or DEX, but high CC-3 levels appeared 6 or 48 hours after a single MFP injection. Simultaneous administration of the agonist-antagonist combination (D+M) partially prevented CC-3 rise at 6 hours, but not at 48 hours (Fig. 1B).

Since appearance of the apoptosis executor CC-3 could reflect an exacerbation of the high sensitivity of Balb-c mice to environmental light, we repeated this experiment in C57Bl6/J mice, which are resistant to light injury. MFP also determined the appearance of CC-3 in this strain, and simultaneous DEX administration prevented CC-3 rise at 6 hours (not shown).

Effects of DEX and MFP on Bcl-X_L and Bax

Bcl-X_L increased 6 and 48 hours after DEX treatment, but this antiapoptotic molecule was not detected in extracts from MFP- or D+M–treated mice (Table 2). A higher DEX dose (10 mg/kg), which induced a higher Bcl-X_L increase (11,720 ± 180 pixels, $n = 4$), did not prevent this effect of MFP (Fig. 2).

Control retinas displayed Bcl-X_L immunoreactivity in all their strata. In the outer retina, immunoreactivity was concentrated at the inner segments (Fig. 3A). Strong immunostaining also appeared in the ganglion cell layer (GCL) and inner nuclear layer (INL). DEX treatment increased immunoreactivity, particularly at the level of the inner segments (Fig. 3B). By contrast, Bcl-X_L immunoreactivity completely disappeared after MFP injection (Fig. 3C). Only weak immunoreactivity showed in D+M retinas, mainly at the level of the GCL (Fig. 3D). Similar staining patterns appeared after 6 and 48 hours of treatment.

Bax and Bcl-X_L showed opposite responses (Table 2). Bax increased 7- to 10-fold above control values at 6 and 48 hours after a single MFP injection ($P < 0.001$). Large Bax increases also occurred in mice receiving the combined D+M. Statistically significant differences between MFP and D+M appeared at 6 hours ($P < 0.01$), but were no longer present after 48 hours. In animals receiving MFP, with or without DEX, the Bcl-X_L/Bax ratios approached 0.

DNA Damage and Repair

Neither control nor DEX-treated retinas showed TUNEL$^+$ nuclei. Only a few TUNEL$^+$ nuclei could be seen 2 hours after MFP administration, but large numbers were present after 6 and 48 hours. TUNEL$^+$ nuclei were selectively found in the ONL. Quantitative analysis did not detect differences in TUNEL$^+$ nuclei density between 6 or 48 hours. D+M retinas did not show TUNEL$^+$ nuclei at 2 or 6 hours but displayed some positive nuclei after 48 hours (Fig. 4).

Fragmented DNA can be repaired by complex mechanisms involving the phosphorylation of histone 2AX. The phosphorylated isoform (p-H2AX) accumulates near to DNA double-strand breaks and serves as a marker of DNA damage and repair.[26] Control and DEX-treated retinas showed no p-H2AX. By contrast, p-H2AX appeared 6 hours after MFP administration, and its levels were even higher 48 hours after pharmacological intervention. Combined D+M administration did not avoid appearance of p-H2AX, but levels were lower than with MFP alone (Fig. 5).

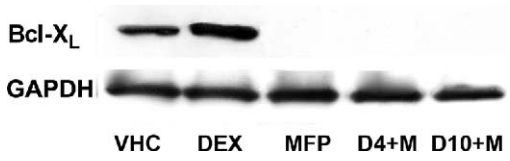

Figure 2. A proteinogram showing Bcl-X_L changes 48 hours after administration of MFP with two different DEX doses: D4, (4 mg/kg, as in previous experiments) and D10 (10 mg/kg). Although DEX (4 mg/kg) increased Bcl-X_L control values, no bands were observed in extracts from MFP, D4+M, or D10+M retinas. See also Table 2.

Table 2. Levels of Bax and Bcl-X_L Proteins 6 and 48 Hours after Pharmacological Intervention

Time	Protein	VHC	DEX	MFP	D+M
6 hours	Bcl-X_L	5223 ± 163	7574 ± 420*	ND*	ND*
	Bax	1933 ± 401	3659 ± 603	14,670 ± 108*	10,720 ± 51*
	Bcl-X_L/Bax	2.70	2.07	≤0.007	≤0.009
48 hours	Bcl-X_L	6902 ± 433	9946 ± 415*	ND*	ND*
	Bax	1987 ± 415	4285 ± 728	20,080 ± 3,033*	18,600 ± 2,542*
	Bcl-X_L/Bax	3.47	2.73	≤0.005	≤0.005

Area of Western blot bands (pixels, mean ± SE, $n = 4$) was compared with ANOVA, followed by Tukey's test. ND, not detected.
* Differences with VHC values were statistically significant ($P < 0.001$).

Table 3. Thickness of the ONL 7 Days after Pharmacological Intervention

Measure	VHC	DEX	MFP	D+M
Total AUC, μm²	188 ± 2	186 ± 6	127 ± 4*	181 ± 5
Temporal AUC, μm²	92 ± 1	91 ± 1	49 ± 3*	88 ± 3
Thickness at first temporal point, μm	46 ± 1	46 ± 1	27 ± 1*	33 ± 2* †

The AUCs representing the ONL thickness were compared by one-way ANOVA followed by Tukey's test. Values are given as mean ± SE ($n = 4$).
* Differences with VHC values were statistically significant, $P < 0.001$.
† Difference with MFP value was statistically significant, $P < 0.05$.

Long-Term Effects of a Single MFP Injection

As an index of photoreceptor demise, we measured changes in the thickness of the ONL using seriate sections stained with Neutral Red. Initially, a blinded operator made a systematic inspection comparing the thickness of the ONL with that of the INL. In control retinas, the ONL was always wider than the INL. We considered that damage existed when the ONL was equal to or thinner than the INL (Fig. 6). These findings are shown as a normal cylindrical projection of the retina, with meridians mapping to equidistant vertical lines (Fig. 7A). No structural alterations appeared in retinas fixed 6 hours after the pharmacological interventions. After 48 hours, the ONL of MFP and D+M retinas showed low-grade lesions that occupied 18.2% ± 1.7% of the total area in MFP retinas, and only 4.9% ± 2.5% of the total area in D+M retinas (*t*-test, $P < 0.005$). Control (VHC injection) and DEX retinas showed no damage.

To test for delayed MFP effects on photoreceptor survival, mice were fixed 7 days after pharmacological intervention. As before, control and DEX retinas presented no detectable damage. In MFP retinas, 48.9% ± 3.0% of the total retinal area showed some degree of photoreceptor nuclei loss. Affected areas in MFP retinas were larger than in D+M retinas (*t*-test, $P < 0.002$). Severe lesions appeared only in 7-day MFP retinas (Fig. 6D), where they occupied almost half of the affected area (42.8% ± 1.7%). This value was statistically different from 0 (*t*-test for one sample, $P < 0.002$). In addition, we measured the thickness of the ONL in equatorial sections (Fig. 7B). Graphs indicated a large decrease in MFP retinas, most evident in the temporal hemisphere. As shown by areas under the curve (AUCs), there was a significant decrease of the ONL thickness in MFP-treated mice (Table 3). We did not find significant differences between the AUCs of control and D+M retinas; however, the thickness at the first point of the temporal hemisphere was significantly lower in D+M than in control or MFP retinas, consistent with the small change detected in our qualitative evaluation.

Two days after administration of DEX, MFP, or their combination, RHO levels were not statistically different from those found in control retinas (Fig. 8A); however, after 7 days, MFP retinas showed a third of the RHO protein found in control (VHC) retinas. Levels in mice subjected to D+M treatment were not statistically different from those in mice that had received a single MFP injection (Fig. 8B).

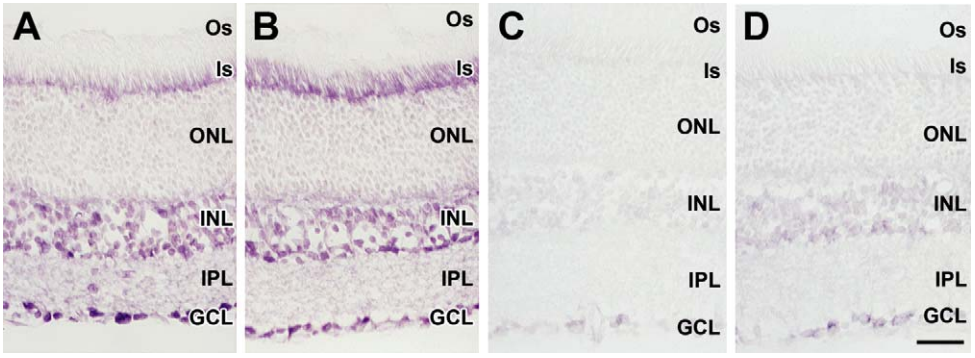

Figure 3. Bcl-X_L immunoreactivity in cryosections from retinas fixed 6 hours after pharmacological interventions. (**A**) In control retinas, Bcl-X_L immunoreactivity concentrated in the GCL, the INL, and the inner segments (Is). (**B**) Inner segment immunoreactivity increased after DEX treatment. (**C**) No immunoreactivity appeared after MFP injection. (**D**) After the combined treatment, weak Bcl-X_L immunoreactivity remained in the GCL and the INL. *Scale bar,* 40 μm (**A–D**).

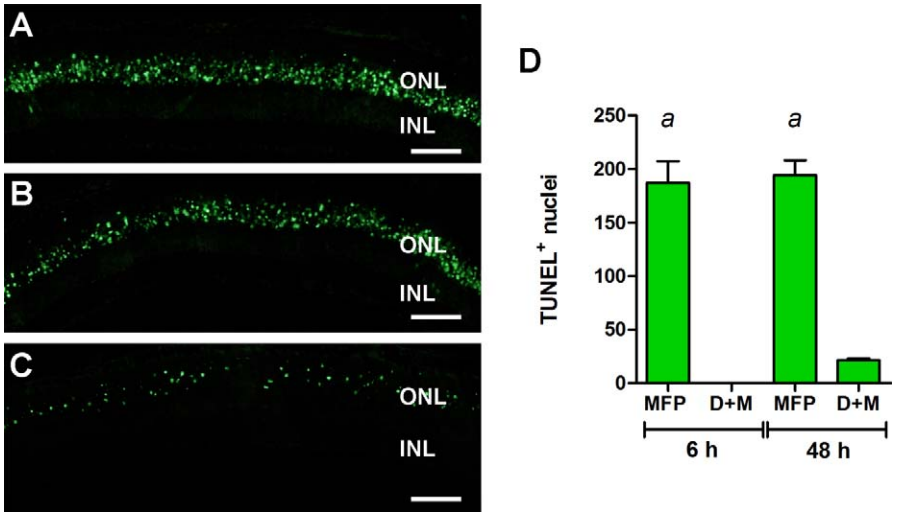

Figure 4. (**A–C**) These composite images of para-equatorial retinal sections show the extent of TUNEL reactivity under different experimental conditions. (**A**) Six hours after MFP injection, large numbers of TUNEL$^+$ nuclei appeared in both retinal hemispheres, nasal and temporal. (**B**) A similar pattern of TUNEL$^+$ nuclei distribution showed 48 hours after MFP administration. (**C**) By contrast, 48 hours after D+M treatment, retinas displayed a small amount of TUNEL$^+$ nuclei. *Scale bars*, 50 μm. (**D**) Quantitative analysis of TUNEL$^+$ nuclei density showed that retinas displayed the same high density 6 and 48 hours after MFP injections. No TUNEL$^+$ nuclei appeared 6 hours after D+M injections, whereas a very low amount was present 48 hours after the combined treatment. Density is expressed as nuclei per 250 μm of ONL (mean ± SE, from 3 retinas, 4 fields per section, $n = 12$).

Adrenalectomy

Retinas from AdrX and sham-operated mice were studied 6 and 48 hours after surgery. Retinas from sham-operated mice never showed TUNEL$^+$ nuclei. On the contrary, all AdrX retinas showed TUNEL$^+$ nuclei that selectively appeared in the ONL. Damaged nuclei were more numerous at 48 hours than at 6 hours after AdrX. TUNEL staining pattern at 48 hours resembled that observed 48 hours after MFP administration (Fig. 9).

Discussion

Glucocorticoids are involved in most cell- and tissue-signaling networks of the organism. They can affect every organ system and regulate important survival responses, such as the behavioral and physical response to stress and disease, the inflammatory reaction, the process of sleep, growth, and reproduction.[27] Within the retina, glucocorticoids are well known by their protective effects after retinal light damage[28]; however, they also modulate the electroretinogram of non-injured retinas,[29,30] suggesting that they could also be important for nonstressed retinas.

Glucocorticoids and Glucocorticoid Receptors in Cell Death and Survival

Understanding the role of glucocorticoids in the retina, as in other neural and non-neural tissues, requires a brief description of the complexity of glucocorticoid receptor (GR) isoforms.[27,31] Alternative splicing of the GR gene transcript generates two C-terminal glucocorticoid receptor isoforms: GRα and GR. In addition, this gene has several initiation sites, giving rise to various isoforms of different length. In the bound state, GRα translocates to the nucleus and binds to glucocorticoid response elements (GREs). GRα may also inhibit key transcription factors, such as nuclear factor-κB (NF-κB) and activator protein-1 (AP-1).[32] MFP is a partial agonist of GRα that allows nuclear translocation of the receptor. The conformational change triggered by association to MFP prevents binding of coactivators and activates recruiting of corepressors.[33] By contrast, GRβ has a unique ligand-binding domain that does not associate with known glucocorticoids and behaves as a dominant negative inhibitor of GRα.[31] Some studies, however, suggest that GRβ

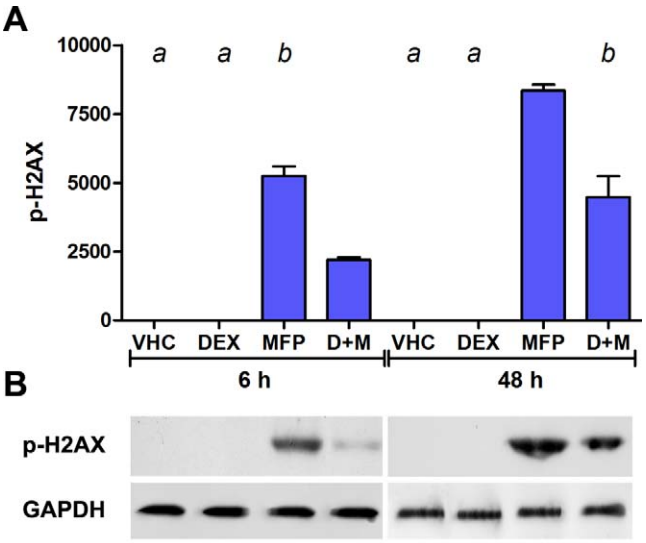

Figure 5. (**A**) Quantitative analysis of p-H2AX Western blots from retinal extracts obtained 6 and 48 hours after pharmacological intervention ($n = 3$; ANOVA, $P < 0.0001$). Differences between columns displaying the same letter were not statistically significant. No p-H2AX was detected in control retinas (VHC), or in those from DEX-treated mice. High levels appeared 6 hours after MFP injection (MFP versus VHC o DEX, $P < 0.001$) and were partially prevented by simultaneous DEX treatment (D+M versus MFP, $P < 0.001$). Higher levels appeared in MFP and D+M retinas after 48 hours (MFP-6 vs. 48, $P < 0.001$; D+M-6 vs. 48, $P < 0.01$). However, D+M at 48 hours was not statistically different from MFP at 6 hours. (**B**) p-H2AX and GAPDH proteinograms at 6 and 48 hours after pharmacological interventions.

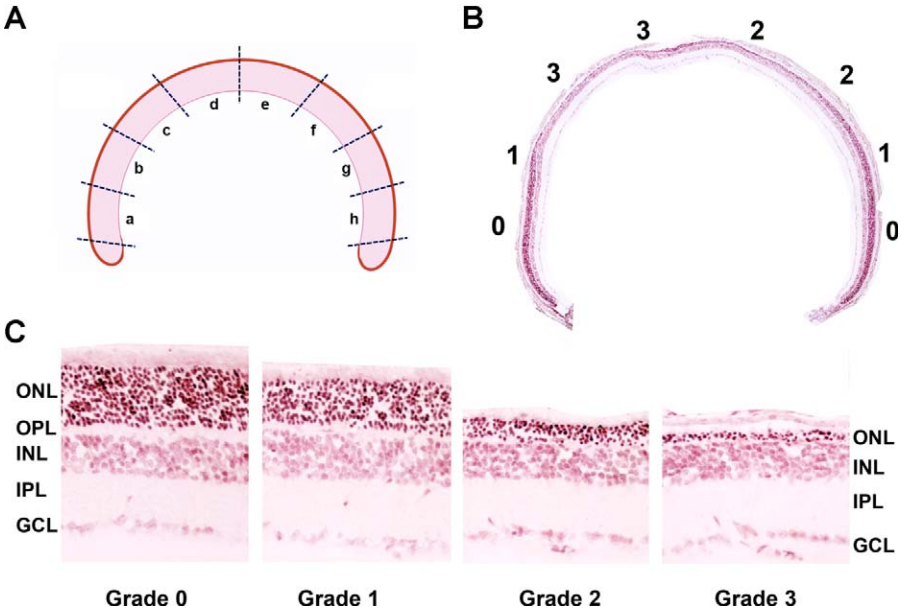

Figure 6. (**A**) A schematic drawing of a retinal section shows the points where we evaluated the ONL. (**B**) This retinal section, stained with Neutral Red, corresponds to a mouse that received MFP 7 days before fixation. *Numbers* indicate the ONL rating from 0 (no damage) to 3 (severe damage). (**C**) Images of the ONL ranked according to damage: 0, the ONL was thicker than the INL; 1, the ONL had the same thickness as the INL; 2, the ONL was thinner than the INL; 3, only 1 to 3 nuclear rows remained in the ONL.

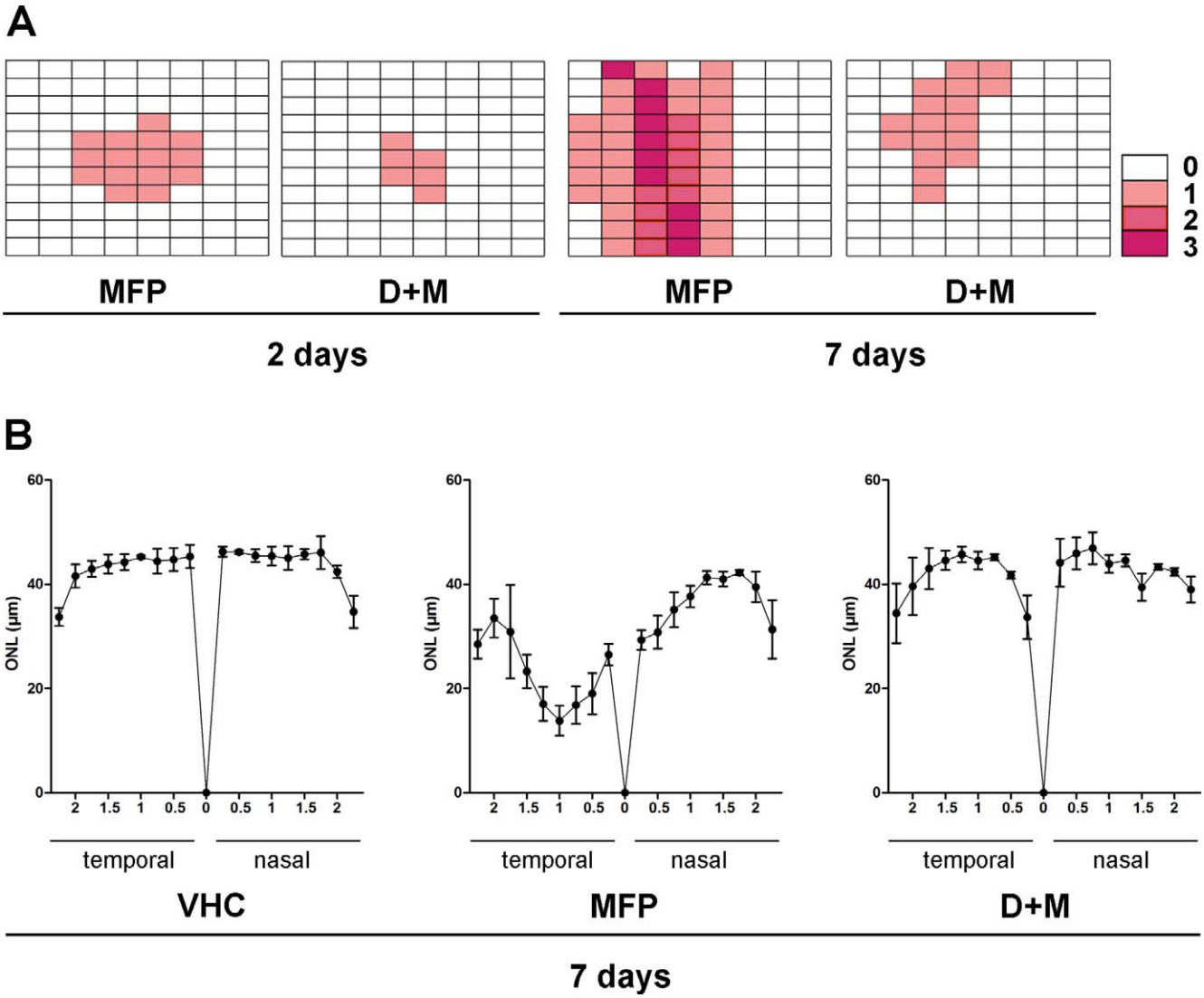

FIGURE 7. (**A**) These four graphs correspond to normal cylindrical projections of retinas at 2 and 7 days of treatment with MFP and D+M. Degree of damage at each point is indicated by a color code (*right lower corner*). Grade 1 lesions appeared after 2 days, the affected area being significantly larger after MFP than after D+M injections. Lesions of grades 2 and 3 were present only in MFP retinas 7 days after treatment. At this time, D+M retinas only showed grade 1 lesions. (**B**) Measurement of the ONL thickness in sections passing through the optic nerve head showed a normal pattern in control animals (VHC). After MFP injection, the temporal hemisphere presented a large lesion. Only a small lesion was detected 7 days after D+M injections (statistical comparisons are described in Table 3).

isoforms might have intrinsic, GRα-independent, transcriptional activity, possibly modulated by MFP binding.[34]

Evidence demonstrating the role of glucocorticoids in cell survival and death is plentiful, particularly since glucocorticoid-dependent apoptosis is one of the mainstays of cancer treatment. Their role in brain and retina has multiple facets, as different neuronal phenotypes respond in opposite fashion.[35–38] The diverse roles of GRα on cell death and survival depend on differential modulation of pro- and antiapoptotic Bcl-2 family members.[39] As previously stated, the prosurvival effect of glucocorticoids is associated with increased expression of Bcl-X_L,[17] the antiapoptotic molecule preferentially expressed by adult central and retinal neurons.[40] Evidence indicates that Bcl-X_L blocks Bax translocation to the mitochondria[41]; thus, we evaluated DEX and MFP effects on these two molecules.

Early Effects of DEX and MFP

Briefly, DEX significantly increased retinal Bcl-X_L, as it occurs in other tissues where glucocorticoids have antiapoptotic actions.[18] A similar pattern appeared after 48 hours, although Bcl-X_L levels in DEX-treated animals were higher than after 6 hours. Photoreceptor inner segments, which contain a large amount of mitochondria, showed the largest DEX-induced increase of Bcl-X_L immunoreactivity. Thus, Bcl-X_L modulation might have some primary influence on photoreceptor functions. DEX also induced a slight increase of Bax, reflected in a decreasing tendency of the Bcl-X_L/Bax ratio in DEX-treated retinas. No evidence of cell death or DNA repair was found in control or DEX-treated retinas.

By contrast, MFP depleted Bcl-X_L and at the same time increased Bax levels, with Bcl-X_L/Bax ratios approaching 0, both at 6 and 48 hours. Photoreceptor injury was a very early phenomenon, with the first ONL TUNEL$^+$ nuclei appearing within 2 hours of MFP administration. At 6 and 48 hours after MFP injection, TUNEL$^+$ nuclei consistently appeared in the ONL of every retinal area, excepting the marginal zone. They were not found in any other retinal layer. Rising levels of CC-3 provided further evidence of retinal injury. Damage was accompanied by the activation of DNA repair mechanisms, as denoted by the accumulation of p-H2AX.[26]

Structural damage of the ONL only became apparent 48 hours after MFP injection, with significant loss of photoreceptor nuclei showing 7 days after the single MFP injection. Repair mechanisms might explain why photoreceptor loss at 7 days was mainly restricted to the temporal hemisphere, whereas in early stages, TUNEL$^+$ nuclei appeared in every retinal region. At 48 hours, ONL lesions were very small and localized in the central retina. This explains why no decrease of RHO appeared at this stage. By contrast, a significant decrease of RHO levels appeared after 7 days, when photoreceptors had disappeared in approximately half of the retina. The course of RHO changes suggests that lesion of the outer segments would be a secondary effect of photoreceptor death and not its cause, as in light-induced retinal degeneration.[16,28]

Interactions between DEX and MFP

Combined administration of DEX and MFP (D+M) significantly reduced retinal damage. DEX prevented increase of CC-3 levels at 6 hours but not at 48 hours after D+M injections. Similarly, animals subjected to D+M treatment did not show TUNEL$^+$ nuclei at 6 hours, but displayed a considerable amount of injured nuclei after 48 hours, in spite of the second DEX injection. Accumulation of p-H2AX followed the same pattern, with levels increasing during the second day of the combined treatment. p-H2AX buildup is proportional to the amount of DNA breaks,[42] indicating that DEX prevented MFP-induced double-strand breaks. Reduction of caspase-3 activation would reduce DNA

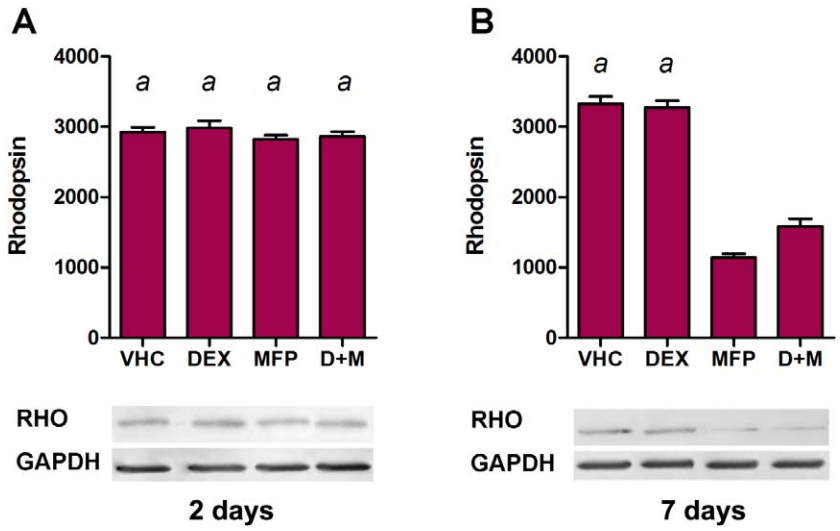

FIGURE 8. (**A**) *Bars* indicate levels of RHO protein 2 days after pharmacological intervention. No significant changes were detected ($n = 3$). (**B**) Seven days after treatment, MFP retinas showed reduced RHO protein levels (MFP versus DEX or VHC, $P < 0.001$; $n = 3$). A significant reduction also appeared in D+M retinas (D+M versus DEX or VHC, $P < 0.001$; $n = 3$), but RHO levels were higher in D+M than in MFP mice ($P < 0.01$; $n = 3$).

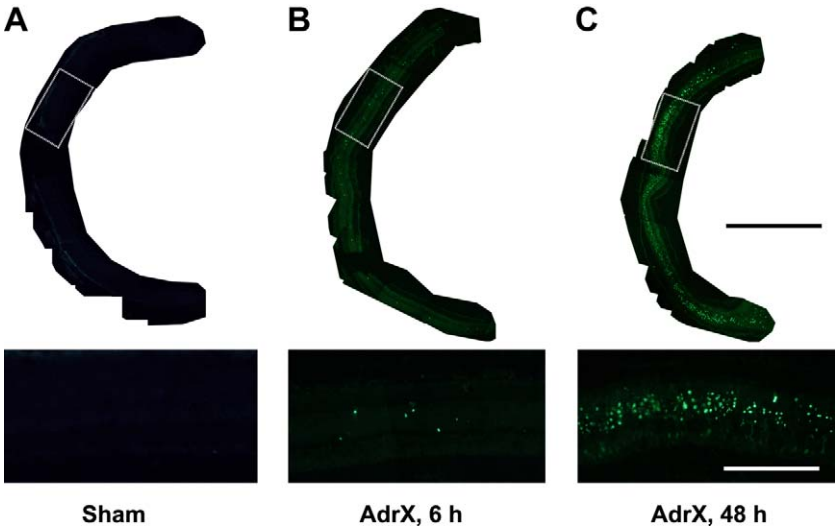

Figure 9. These composite images illustrate TUNEL reactivity in the retina of AdrX and sham-operated mice. The *inset below each image* corresponds to the *boxed area* of each image. (**A**) A section through the retina of a sham-operated mouse shows no detectable TUNEL$^+$ nuclei, as can be confirmed in the *inset*. (**B**) A few TUNEL$^+$ nuclei showed in the ONL, just 6 hours after AdrX. (**C**) A larger number of TUNEL$^+$ nuclei appeared 48 hours after AdrX. The *inset* shows that TUNEL$^+$ nuclei were selectively located in the ONL. *Scale bars* (for all figures): photomontages, 200 μm; insets, 50 μm.

fragmentation, but glucocorticoids could also interact directly with p53.[43] This might be an important antiapoptotic mechanism in the retina, as DEX prevented photoreceptor death without improving the MFP-induced Bcl-X_L depletion.

In spite of the TUNEL and CC-3 increases during the second day of the experiment, mice subjected to the combined treatment showed little ONL damage at 7 days after MFP injection; however, their RHO levels resembled those of MFP-treated animals.

These findings might be explained by the long half-life of MFP.[44] On the other hand, they might reflect other effects of this molecule, perhaps dependent on GRβ isoforms.[45,46] MFP also antagonizes progesterone receptors,[47] which are also involved in Bcl-X_L upregulation[48,49] and have a role in photoreceptor protection.[50,51] Our present findings, however, suggest that glucocorticoid signaling is required for photoreceptor survival. We used male mice, where progesterone levels are low,[52] and survival was promoted by DEX, a selective ligand of GRα, with very low affinity for mineralocorticoid and progesterone receptors.[1,53] Most important, we induced selective photoreceptor death by AdrX, supporting the involvement of glucocorticoids in photoreceptor maintenance.

MFP and Photoreceptor Death

Present findings indicate that MFP is a potent and selective toxin for murine photoreceptors. This effect cannot be explained by the dose, because we used a single 10-mg/kg injection. By contrast, higher amounts (20–100 mg/kg) and longer treatments are often reported in the literature.[54–57]

Lack of Bcl-X_L increases photoreceptor vulnerability to some stressors, but would not be a direct cause of photoreceptor damage.[58] MFP induced disappearance of Bcl-X_L in all retinal cell phenotypes; however, only photoreceptors were damaged after MFP administration. On the other hand, photoreceptors are the highest oxygen-consuming cells in the organism and are particularly susceptible to oxidative stress.[59] This property could perhaps explain their extreme sensitivity to MFP, as glucocorticoids are involved in the clearance of oxidative damage in neurons.[60]

Main Conclusions

Both MFP and AdrX provoked selective damage of photoreceptor nuclei in male mice under standard illumination conditions. DEX prevented damage, suggesting that adrenal steroids might be essential for photoreceptor survival in a normal environment.

MFP is currently approved in several countries for termination of pregnancy, and has been recommended for emergency contraception, leiomyomas, and endometriosis.[61] Its use as an antidepressant and in central serous chorioretinopathy has also been proposed.[62,63] Daily doses of 200 to 600 mg are recommended but, to our knowledge, visual adverse effects have not been reported. Thus, massive photoreceptor damage as we have seen in two different strains of mice probably would not occur in humans; however, DNA fragmentation could determine selective accumulation of mutations in photoreceptor nuclei, perhaps enhancing degenerative phenomena produced by other causes.

On the other hand, confirmation of an essential role of glucocorticoids (or other adrenal steroids) in photoreceptor homeostasis, would support their use in combination with more specific agents, for prevention or treatment of retinal degenerations.

Acknowledgments

We are grateful to Soledad Arregui, Guillermo Gastón, and Marcos Cabrera for their skillful technical assistance.

References

1. Edelman JL. Differentiating intraocular glucocorticoids. *Ophthalmologica*. 2010;224:25–30.
2. Yu-Wai-Man P, Griffiths PG. Steroids for traumatic optic neuropathy. *Cochrane Database Syst Rev*. 2011;1:CD006032.
3. Campochiaro PA, Hafiz G, Shah SM, et al. Sustained ocular delivery of fluocinolone acetonide by an intravitreal insert. *Ophthalmology*. 2010;117:1393–1399.e3.

4. Aref AA, Scott IU. Management of macular edema secondary to central retinal vein occlusion: an evidence-based. *Adv Ther*. 2011;28:40–50.
5. Boscia F, Furino C, Dammacco R, Ferreri P, Sborgia L, Sborgia C. Intravitreal triamcinolone acetonide in refractory pseudophakic cystoid macular edema: functional and anatomic results. *Eur J Ophthalmol*. 2005;15:89–95.
6. Jonas JB, Kreissig I, Degenring R. Intravitreal triamcinolone acetonide for treatment of intraocular proliferative, exudative, and neovascular diseases. *Prog Retin Eye Res*. 2005;24:587–611.
7. Sallam A, Taylor SR, Lightman S. Review and update of intraocular therapy in noninfectious uveitis. *Curr Opin Ophthalmol*. 2011;22:517–522.
8. Horgan N, Shields CL, Mashayekhi A, Shields JA. Classification and treatment of radiation maculopathy. *Curr Opin Ophthalmol*. 2010;21:233–238.
9. Augustin A. Triple therapy for age-related macular degeneration. *Retina*. 2009;29:S8–11.
10. Fu J, Lam TT, Tso MO. Dexamethasone ameliorates retinal photic injury in albino rats. *Exp Eye Res*. 1992;54:583–594.
11. Wenzel A, Grimm C, Seeliger MW, et al. Prevention of photoreceptor apoptosis by activation of the glucocorticoid receptor. *Invest Ophthalmol Vis Sci*. 2001;42:1653–1659.
12. Gu D, Beltran WA, Pearce-Kelling S, Li Z, Acland GM, Aguirre GD. Steroids do not prevent photoreceptor degeneration in the light-exposed T4R rhodopsin mutant dog retina irrespective of AP-1 inhibition. *Invest Ophthalmol Vis Sci*. 2009;50:3482–3494.
13. Brown J Jr, Hacker H, Schuschereba ST, Zwick H, Lund DJ, Stuck BE. Steroidal and nonsteroidal antiinflammatory medications can improve photoreceptor survival after laser retinal photocoagulation. *Ophthalmology*. 2007;114:1876–1883.
14. Takahashi K, Lam TT, Fu J, Tso MO. The effect of high-dose methylprednisolone on laser-induced retinal injury in primates: an electron microscopic study. *Graefes Arch Clin Exp Ophthalmol*. 1997;235:723–732.
15. Glybina IV, Kennedy A, Ashton P, Abrams GW, Iezzi R. Photoreceptor neuroprotection in RCS rats via low-dose intravitreal sustained-delivery of fluocinolone acetonide. *Invest Ophthalmol Vis Sci*. 2009;50:4847–4857.
16. Cubilla MA, Castañeda MM, Bachor TP, Suburo AM. Glucocorticoid-dependent mechanisms in photoreceptor survival. *Adv Exp Med Biol*. 2012;723:101–106.
17. Viegas LR, Hoijman E, Beato M, Pecci A. Mechanisms involved in tissue-specific apoptosis regulated by glucocorticoids. *J Steroid Biochem Mol Biol*. 2008;109:273–278.
18. Kfir-Erenfeld S, Sionov RV, Spokoini R, Cohen O, Yefenof E. Protein kinase networks regulating glucocorticoid-induced apoptosis of hematopoietic cancer cells: fundamental aspects and practical considerations. *Leuk Lymphoma*. 2010;51:1968–2005.
19. Yang N, Zhang H, Si-Ma H, et al. Dexamethasone decreases hepatocellular carcinoma cell sensitivity to cisplatin-induced apoptosis. *Hepatogastroenterology*. 2011;58:1730–1735.
20. Scoltock AB, Heimlich G, Cidlowski JA. Glucocorticoids inhibit the apoptotic actions of UV-C but not Fas ligand in hepatoma cells: direct evidence for a critical role of Bcl-xL. *Cell Death Differ*. 2007;14:840–850.
21. Nieuwenhuis B, Luth A, Kleuser B. Dexamethasone protects human fibroblasts from apoptosis via an S1P3-receptor subtype dependent activation of PKB/Akt and Bcl XL. *Pharmacol Res*. 2010;61:449–459.
22. Almeida OF, Conde GL, Crochemore C, et al. Subtle shifts in the ratio between pro- and antiapoptotic molecules after activation of corticosteroid receptors decide neuronal fate. *FASEB J*. 2000;14:779–790.
23. Foley LP. Common surgical procedures in rodents. In: Reuter JD, Suckow MA, eds. *Laboratory Animal Medicine and Management*. Ithaca, NY: International Veterinary Information Service; 2005:B2515.0605.
24. Torbidoni V, Iribarne M, Ogawa L, Prasanna G, Suburo AM. Endothelin-1 and endothelin receptors in light-induced retinal degeneration. *Exp Eye Res*. 2005;81:265–275.
25. Tanito M, Kaidzu S, Anderson RE. Delayed loss of cone and remaining rod photoreceptor cells due to impairment of choroidal circulation after acute light exposure in rats. *Invest Ophthalmol Vis Sci*. 2007;48:1864–1872.
26. van Attikum H, Gasser SM. Crosstalk between histone modifications during the DNA damage response. *Trends Cell Biol*. 2009;19:207–217.
27. Chrousos GP, Kino T. Intracellular glucocorticoid signaling: a formerly simple system turns stochastic. *Sci STKE*. 2005;pe48.
28. Organisciak DT, Vaughan DK. Retinal light damage: mechanisms and protection. *Prog Retin Eye Res*. 2010;29:113–134.
29. Zimmerman TJ, Dawson WW, Fitzgerald CR. ERG in human eyes following oral adrenocorticoids. *Invest Ophthalmol*. 1973;12:777–779.
30. Abraham I, Palhalmi J, Szilagyi N, Juhasz G. Glucocorticoids alter recovery processes in the rat retina. *Neuroreport*. 1998;9:1465–1468.
31. Oakley RH, Cidlowski JA. Cellular processing of the glucocorticoid receptor gene and protein: new mechanisms for generating tissue specific actions of glucocorticoids. *J Biol Chem*. 2011;286:3177–3184.
32. Zanchi NE, Filho MA, Felitti V, Nicastro H, Lorenzeti FM, Lancha AH Jr. Glucocorticoids: extensive physiological actions modulated through multiple mechanisms of gene regulation. *J Cell Physiol*. 2010;224:311–315.
33. Schoch GA, D'Arcy B, Stihle M, et al. Molecular switch in the glucocorticoid receptor: active and passive antagonist conformations. *J Mol Biol*. 2010;395:568–577.
34. Lewis-Tuffin LJ, Jewell CM, Bienstock RJ, Collins JB, Cidlowski JA. Human glucocorticoid receptor beta binds RU-486 and is transcriptionally active. *Mol Cell Biol*. 2007;27:2266–2282.
35. McEwen BS. Glucocorticoids, depression, and mood disorders: structural remodeling in the brain. *Metabolism*. 2005;54:20–23.
36. Dutt M, Tabuena P, Ventura E, Rostami A, Shindler KS. Timing of corticosteroid therapy is critical to prevent retinal ganglion cell loss in experimental optic neuritis. *Invest Ophthalmol Vis Sci*. 2010;51:1439–1445.
37. Smit-McBride Z, Modjtahedi SP, Cessna CT, Telander DG, Hjelmeland LM, Morse LS. In vivo gene expression profiling of retina postintravitreal injections of dexamethasone and triamcinolone at clinically relevant time points for patient care. *Invest Ophthalmol Vis Sci*. 2011;52:8965–8978.
38. Noguchi KK, Walls KC, Wozniak DF, Olney JW, Roth KA, Farber NB. Acute neonatal glucocorticoid exposure produces selective and rapid cerebellar neural progenitor cell apoptotic death. *Cell Death Differ*. 2008;15:1582–1592.
39. Amaral JD, Sola S, Steer CJ, Rodrigues CM. Role of nuclear steroid receptors in apoptosis. *Curr Med Chem*. 2009;16:3886–3902.
40. Levin LA, Schlamp CL, Spieldoch RL, Geszvain KM, Nickells RW. Identification of the bcl-2 family of genes in the rat retina. *Invest Ophthalmol Vis Sci*. 1997;38:2545–2553.
41. He L, Perkins GA, Poblenz AT, et al. Bcl-xL overexpression blocks bax-mediated mitochondrial contact site formation and apoptosis in rod photoreceptors of lead-exposed mice. *Proc Natl Acad Sci U S A*. 2003;100:1022–1027.
42. Redon CE, Nakamura AJ, Martin OA, Parekh PR, Weyemi US, Bonner WM. Recent developments in the use of gamma-H2AX

as a quantitative DNA double-strand break biomarker. *Aging (Albany NY)*. 2011;3:168–174.

43. Aziz MH, Shen H, Maki CG. Glucocorticoid receptor activation inhibits p53-induced apoptosis of MCF10Amyc cells via induction of protein kinase C{epsilon}. *J Biol Chem*. 2012; 287:29825–29836.
44. Heikinheimo O, Raivio T, Honkanen H, Ranta S, Janne OA. Termination of pregnancy with mifepristone and prostaglandin suppresses transiently circulating glucocorticoid bioactivity. *J Clin Endocrinol Metab*. 2003;88:323–326.
45. Kino T, Manoli I, Kelkar S, Wang Y, Su YA, Chrousos GP. Glucocorticoid receptor (GR) beta has intrinsic, GRalpha-independent transcriptional activity. *Biochem Biophys Res Commun*. 2009;381:671–675.
46. Ligr M, Li Y, Logan SK, et al. Mifepristone inhibits GRbeta coupled prostate cancer cell proliferation. *J Urol*. 2012;188: 981–988.
47. Beck CA, Estes PA, Bona BJ, Muro-Cacho CA, Nordeen SK, Edwards DP. The steroid antagonist RU486 exerts different effects on the glucocorticoid and progesterone receptors. *Endocrinology*. 1993;133:728–740.
48. Morrissy S, Xu B, Aguilar D, Zhang J, Chen QM. Inhibition of apoptosis by progesterone in cardiomyocytes. *Aging Cell*. 2010;9:799–809.
49. Pecci A, Scholz A, Pelster D, Beato M. Progestins prevent apoptosis in a rat endometrial cell line and increase the ratio of bcl-XL to bcl-XS. *J Biol Chem*. 1997;272:11791–11798.
50. Doonan F, O'Driscoll C, Kenna P, Cotter TG. Enhancing survival of photoreceptor cells in vivo using the synthetic progestin Norgestrel. *J Neurochem*. 2011;118:915–927.
51. Cubilla MA, Bachor TP, Bermudez V, Marquioni MD, Suburo AM. Progesterone protects photoreceptors from light-induced damage. *ARVO Meeting Abstracts*. 2012;53:2565.
52. Frye CA, Llaneza DC. Corticosteroid and neurosteroid dysregulation in an animal model of autism, BTBR mice. *Physiol Behav*. 2010;100:264–267.
53. Issar M, Sahasranaman S, Buchwald P, Hochhaus G. Differences in the glucocorticoid to progesterone receptor selectivity of inhaled glucocorticoids. *Eur Respir J*. 2006;27:511–516.
54. Hill MN, McLaughlin RJ, Pan B, et al. Recruitment of prefrontal cortical endocannabinoid signaling by glucocorticoids contributes to termination of the stress response. *J Neurosci*. 2011;31:10506–10515.
55. Asagami T, Belanoff JK, Azuma J, Blasey CM, Clark RD, Tsao PS. Selective glucocorticoid receptor (GR-II) antagonist reduces body weight gain in mice. *J Nutr Metab*. 2011;2011:235389.
56. Pryce G, Giovannoni G, Baker D. Mifepristone or inhibition of 11beta-hydroxylase activity potentiates the sedating effects of the cannabinoid receptor-1 agonist Delta(9)-tetrahydrocannabinol in mice. *Neurosci Lett*. 2003;341:164–166.
57. Wulsin AC, Herman JP, Solomon MB. Mifepristone decreases depression-like behavior and modulates neuroendocrine and central hypothalamic-pituitary-adrenocortical axis responsiveness to stress. *Psychoneuroendocrinology*. 2010;35:1100–1112.
58. Zheng L, Anderson RE, Agbaga MP, Rucker EB III, Le YZ. Loss of BCL-XL in rod photoreceptors: increased susceptibility to bright light stress. *Invest Ophthalmol Vis Sci*. 2006;47:5583–5589.
59. Cringle SJ, Yu PK, Su EN, Yu DY. Oxygen distribution and consumption in the developing rat retina. *Invest Ophthalmol Vis Sci*. 2006;47:4072–4076.
60. Shuto M, Higuchi K, Sugiyama C, et al. Endogenous and exogenous glucocorticoids prevent trimethyltin from causing neuronal degeneration of the mouse brain in vivo: involvement of oxidative stress pathways. *J Pharmacol Sci*. 2009;110: 424–436.
61. Bouchard P, Chabbert-Buffet N, Fauser BC. Selective progesterone receptor modulators in reproductive medicine: pharmacology, clinical efficacy and safety. *Fertil Steril*. 2011;96: 1175–1189.
62. Schule C, Baghai TC, Eser D, Rupprecht R. Hypothalamic-pituitary-adrenocortical system dysregulation and new treatment strategies in depression. *Expert Rev Neurother*. 2009;9: 1005–1019.
63. Nielsen JS, Jampol LM. Oral mifepristone for chronic central serous chorioretinopathy. *Retina*. 2011;31:1928–1936.